ACS OMEGA

http://pubs.acs.org/journal/acsodf

Article

Berberine Reverses Breast Cancer Multidrug Resistance Based on Fluorescence Pharmacokinetics *In Vitro* and *In Vivo*

Ke Qian,[▽] Chao-yuan Tang,[▽] Li-ying Chen, Shuang Zheng, Yue Zhao, Li-sha Ma, Li Xu, Lu-hui Fan, Jian-dong Yu, Hong-sheng Tan, Ya-lan Sun, Li-li Shen, Yang Lu, Qi Liu, Yun Liu, and Yang Xiong*

Cite This: *ACS Omega* 2021, 6, 10645−10654

Read Online

ACCESS | Metrics & More | Article Recommendations

ABSTRACT: Exploring the mechanism through which berberine (Ber) reverses the multidrug resistance (MDR) of breast cancer is of great importance. Herein, we used the methyl thiazolyl tetrazolium assay to determine the drug resistance and cytotoxicity of Ber and doxorubicin (DOX) alone or in combination on the breast cancer cell line MCF-7/DOX^{Fluc}. The results showed that Ber could synergistically enhance the inhibitory effect of DOX on tumor cell proliferation *in vitro*, and the optimal combination ratio was Ber/DOX = 2:1. Using a luciferase reporter assay system combined with the bioluminescence imaging technology, the efflux kinetics of D-luciferin potassium salt in MCF-7/DOX^{Fluc} cells treated with Ber *in vivo* was investigated. The results showed that Ber could significantly reduce the efflux of D-luciferin potassium salt in MCF-7/DOX^{Fluc} cells. In addition, western blot and immunohistochemistry experiments showed that the expression of P-glycoprotein (P-gp/ABCB1) and multidrug resistance protein 1 (MRP1/ABCC1) in MCF-7/DOX^{Fluc} cells was downregulated upon Ber treatment. Finally, high-performance liquid chromatography was used to investigate the effect of Ber on DOX tissue distribution *in vivo*, and the results showed that the uptake of DOX in tumor tissues increased significantly when combined with Ber ($P < 0.05$). Thus, the results illustrated that Ber can reverse MDR by inhibiting the efflux function of ATP-binding cassette transporters and downregulating their expression levels.

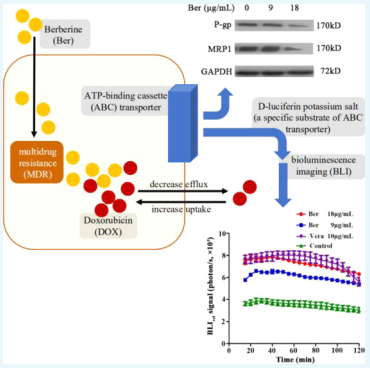

1. INTRODUCTION

Breast cancer is the number one killer of women and is the second-most prevalent cancer worldwide, accounting for about one-fourth of the confirmed female cancer cases.[1] At present, chemotherapy is one of the important means to treat breast cancer. However, the ability of cancer cells to rapidly develop resistance to chemotherapy is the major reason for chemotherapy failure.[2−8] Therefore, the study of tumor multidrug resistance (MDR) has become a major focus within cancer research, with the goal of discovering a method to reverse MDR. According to current research results, the possible mechanisms of MDR include high expression of ATP-binding cassette (ABC) transporters, abnormal enzyme expression, changes in genes and proteins that control apoptosis, and changes in related signaling pathways.[9−13] Multiple mechanisms may co-exist at the same time, or the dominant role may be played by only one mechanism. In recent years, combining traditional Chinese medicine (TCM) with chemotherapeutic drugs to combat MDR has been proposed. TCM can act on multiple components of interest at once, which is likely key to reversing MDR.[14−17]

At present, the research on TCM agents used to reverse MDR cannot unify the reversal effects observed *in vivo* and *in vitro* in tumor cells. It is difficult to establish the correlation of the research results between *in vivo* and *in vitro* because of the different pharmacodynamic evaluation indexes of drugs. *In vitro* experiment drugs directly act on tumor cells; however, the tumor microenvironment *in vivo* is complex and diverse. Therefore, it is necessary to find a specific real-time dynamic monitoring technology or method which could evaluate the drug efficacy on tumor cells, both *in vivo* and *in vitro*. Previously, our team conducted research on the MDR reversal effect of many TCMs in doxorubicin (DOX)-resistant breast cancer *in vitro* by a real-time, quantitative, and dynamic detection method *in vitro*, and berberine (Ber) was chosen. Ber is an active alkaloid extracted from medicinal plants such as *Coptis chinensis*.[18] To investigate whether Ber would keep the MDR reversal effect *in vivo* as *in vitro* and to understand how Ber could reverse MDR, we designed and conducted this study.

Bioluminescence imaging (BLI) is a widely used tool to study the biological process of living animals, and it can directly and sensitively monitor the activity of luciferase gene cells *in vivo*.[19−22] BLI can integrate the firefly luciferase (Fluc) gene into the chromosomal DNA of cells to express luciferase. When its

Received: December 26, 2020
Accepted: March 1, 2021
Published: April 13, 2021

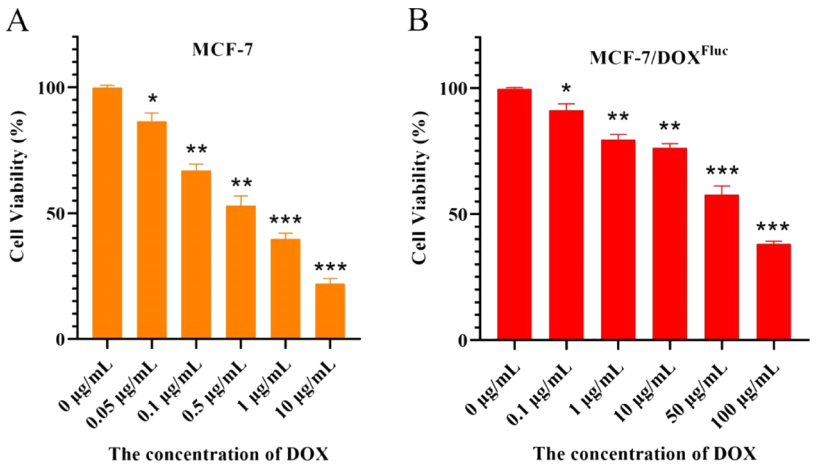

Figure 1. (A) Cell viability of MCF-7, $n = 6$, $\bar{x} \pm s$. * $P < 0.05$, ** $P < 0.01$, *** $P < 0.001$ vs the phosphate-buffered saline (PBS) group. (B) Cell viability of MCF-7/DOX^{Fluc}, $n = 6$, $\bar{x} \pm s$. * $P < 0.05$, ** $P < 0.01$, *** $P < 0.001$ vs the PBS group. Significant differences were assessed using the *t* test. Results are presented as means ± SD.

exogenous specific substrate, fluorescein, is added, either directly into the cell culture media *in vitro* or injected intraperitoneally or intravenously *in vivo*, luminescence can occur within a few minutes. In the presence of ATP and oxygen, the enzyme can emit light only in living cells, and the intensity of light is linearly correlated to the number of labeled cells. Both cells and living animals can be labeled with the luciferase gene. With the help of BLI, the activity of luciferase-expressing cells *in vitro* or *in vivo* can be monitored dynamically.

D-luciferin potassium salt is a specific substrate of the ABC transporter, and its pharmacokinetic (PK) profile in tumor cells is closely related to the function and/or expression of the ABC transporter.[23,24] D-luciferin potassium salt is also a specific substrate for Fluc. When taken into tumor cells, it can be oxidized by luciferase expressed by the tumor cells and then produce photons correlating with the molar amount of luciferin present. Therefore, this method can dynamically monitor the efflux of D-luciferin potassium salt in tumor cells in real time, thus reflecting the dynamic process of the ABC transporter *in vitro* and *in vivo*.[25,26]

In this study, the MCF-7/DOX^{Fluc} cell line with stably overexpressed luciferase was established. Using the luciferase reporter gene system combined with BLI technology, according to the theoretical support that the PK of D-luciferin potassium salt in tumor cells is closely related to the function of the ABC transporter, the PK parameter of D-luciferin potassium salt was evaluated in MCF-7/DOX^{Fluc} cells *in vitro* and *in vivo*. In addition, western blot and immunohistochemistry (IHC) experiments were used to study the effect of Ber on the expression of ABC protein in MCF-7/DOX^{Fluc} cells.

2. RESULTS AND DISCUSSION

2.1. Multiple Drug Resistance of MCF-7/DOX^{Fluc}. The cell viability of MCF-7 and MCF-7/DOX^{Fluc} was calculated (Figure 1A,B). IC_{50} of 0.55 μg/mL for MCF-7 and 72.46 μg/mL for MCF-7/DOX^{Fluc}, giving a multiple drug resistance of MCF-7/DOX^{Fluc} was 131.75.

2.2. Combined Treatment of DOX and Ber Inhibited the Proliferation of MCF-7/DOX^{Fluc} Cells *In Vitro*. To observe the proliferation rate of MCF-7/DOX^{Fluc} cells treated with DOX and Ber alone or in combination, a synergistic ratio of DOX and Ber was calculated. When the combination ratios of Ber and DOX were 1:1, 2:1, 5:1, and 10:1, the IC_{50} values after 48 h were 6.6, 3.2, 4.6, and 6.1 μg/mL, respectively, lower than that of DOX alone (IC_{50} = 12.6 μg/mL, $P < 0.05$) and Ber alone (IC_{50} = 20.0 μg/mL, $P < 0.05$) (Figure 2A). The combination index (CI) values were 1.11, 0.51, 0.76, and 1.70, respectively, and there was statistical difference when the combination ratios were 2:1 and 5:1 ($P < 0.05$) (Figure 2B). These findings indicated that Ber could enhance the inhibitory effect of DOX on cell proliferation through the synergistic effect. The optimal combinatory ratio of Ber to DOX was 2:1.

2.3. Combined Treatment of Ber and DOX Enhanced the Inhibition of MCF-7/DOX^{Fluc} Breast Cancer Xenogeneic Model *In Vivo*. The tumor volume in the group of Ber combined with DOX was smaller than that of other groups (Figure 2C). Compared with the PBS group, the group treated with Ber (10 mg/kg, *i.p.*) or DOX (5 mg/kg, *i.v.*) alone exhibited a mild reduction of tumor growth, whereas the combination of DOX and Ber exhibited significant tumor growth inhibition efficiency ($P < 0.05$) (Figure 2D). The BLI results showed that the quantity of MCF-7/DOX^{Fluc} cells was significantly reduced in the combined group compared with the PBS group ($P < 0.05$). The BLI results showed a decrease in the quantity of MCF-7/DOX^{Fluc} cells treated with either Ber alone (10 mg/kg, *i.p.*) or DOX alone (5 mg/kg, *i.v.*) compared with the PBS group, whereas a significant decrease in the quantity of MCF-7/DOX^{Fluc} cells was observed after DOX and Ber treatment ($P < 0.05$) (Figure 2E). The body weight of nude mice in the DOX group was significantly reduced, maybe because DOX could cause toxicities and side effects. After treated by the combination of Ber and DOX, the weight change of nude mice was similar to that treated by DOX alone (Figure 2F). It seemed that Ber could not reverse the toxic side effects of DOX at a high dose (5 mg/kg). Therefore, the concentration of DOX was decreased from 5 to 2 mg/kg to observe the synergistic effect and the toxicities in a later experiment.

2.4. Ber Could Combine with DOX of Low Dose to Reduce Toxicity *In Vivo*. Compared with the PBS group, the group treated with DOX at a low dose (2 mg/kg, *i.v.*) alone exhibited a mild reduction of tumor growth, whereas DOX (2 mg/kg, *i.v.*) combined with Ber (4 mg/kg, *i.p.*) produced a significant tumor growth inhibition effect, which was similar to the treatment with DOX alone at a high dose (5 mg/kg, *i.v.*) ($P < 0.05$) (Figure 3A). The body weight of nude mice in the DOX group showed a significant decrease compared with that in the

https://doi.org/10.1021/acsomega.0c06288
ACS Omega 2021, 6, 10645−10654

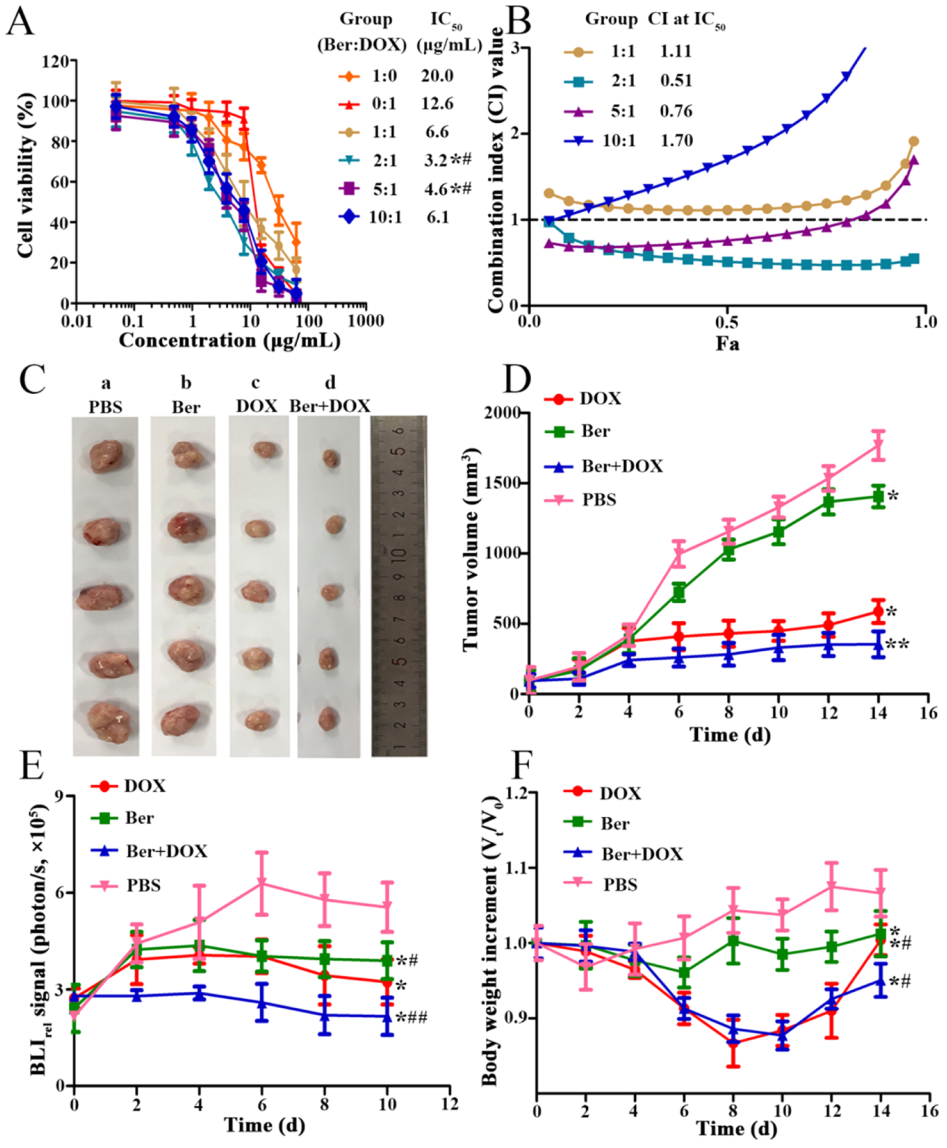

Figure 2. (A) MCF-7/DOX^{Fluc} cells treated by DOX and Ber with different ratios for 48 h. $n = 6, \bar{x} \pm s$. * $P < 0.05$, ** $P < 0.01$ vs the DOX group; $^{\#}$ $P < 0.05$, $^{\#\#}$ $P < 0.01$ vs the Ber group. (B) Synergistic index curve of MCF-7/DOX^{Fluc} cells treated by DOX and Ber in different ratios for 48 h. (C) Tumor volumes of MCF-7/DOX^{Fluc} tumor-bearing nude mice treated by DOX (5 mg/kg, *i.v.*) alone or in combination with Ber (10 mg/kg, *i.p.*). * $P < 0.05$, ** $P < 0.01$ vs the PBS group; $^{\#}$ $P < 0.05$, $^{\#\#}$ $P < 0.01$ vs the DOX group. a: PBS group; b: Ber group; c: DOX group; d: Ber + DOX group. (D) Visual observations of MCF-7/DOX^{Fluc} tumor volumes in each treatment group at the end time point. (E) BLI$_{rel}$ signal photon−time curve of MCF-7/DOX^{Fluc} treated *in vivo* by different drugs after intraperitoneally injecting D-luciferin potassium salt at a dose of 10 mg/kg. (F) Effect of different drugs on the body weight of MCF-7/DOX^{Fluc} tumor-bearing nude mice. * $P < 0.05$, ** $P < 0.01$ vs the PBS group. Significant differences were assessed using one-way ANOVA. Multiple comparisons between the groups were performed using the Tukey method. Results are presented as means ± SD.

PBS group, whereas the body weight in the Ber + DOX group showed no significant decrease, indicating that Ber could reduce the toxicity induced by DOX at a low dose (Figure 3B). The variation in tumor mass showed a similar trend (Figure 3C).

2.5. Ber Inhibited the Function of ABC Transporter in MCF-7/DOX^{Fluc} Cells *In Vitro*. The fluorescence efflux kinetics of D-luciferin potassium salt was monitored by BLI *in vitro* after the MCF-7/DOX^{Fluc} cells were treated by Ber for 48 h. The results showed that Ber could significantly inhibit the efflux of D-luciferin potassium salt (Figure 4A). The fluorescence intensity of MCF-7/DOX^{Fluc} cells treated with the ABCB1 inhibitor (Verapamil (Vera), 10 μg/mL) or Ber in different concentrations (9 and 18 μg/mL) for 48 h was detected by *in vivo* imaging system (IVIS). PK parameters in each group were obtained from the bioluminescent signal intensity of D-luciferin potassium salt, and the area under curve (AUC) and mean residence time (MRT) were fitted into the noncompartment model. The results showed that both Ber and Vera could significantly increase AUC and decrease MRT ($P < 0.001$). These data indicated that Ber could decelerate the clearance and efflux rate of D-luciferin potassium salt in MCF-7/DOX^{Fluc} cells. It meant that Ber could inhibit the function of the ABC transporter and thus reduce the efflux (Table 1).

2.6. Ber Inhibited the Function of ABC Transporters in MCF-7/DOX^{Fluc} Cells *In Vivo*. On the 7th and 14th days after receiving Ber (10 mg/kg, *i.p.*), the MCF-7/DOX^{Fluc} tumor-bearing nude mice were injected with D-luciferin potassium salt (10 μg/mL, *i.p.*), and the luminescence signal was detected by BLI. Within 130 min, the bioluminescence signal value of D-luciferin potassium salt decreased gradually with time, and the

https://doi.org/10.1021/acsomega.0c06288
ACS Omega 2021, 6, 10645−10654

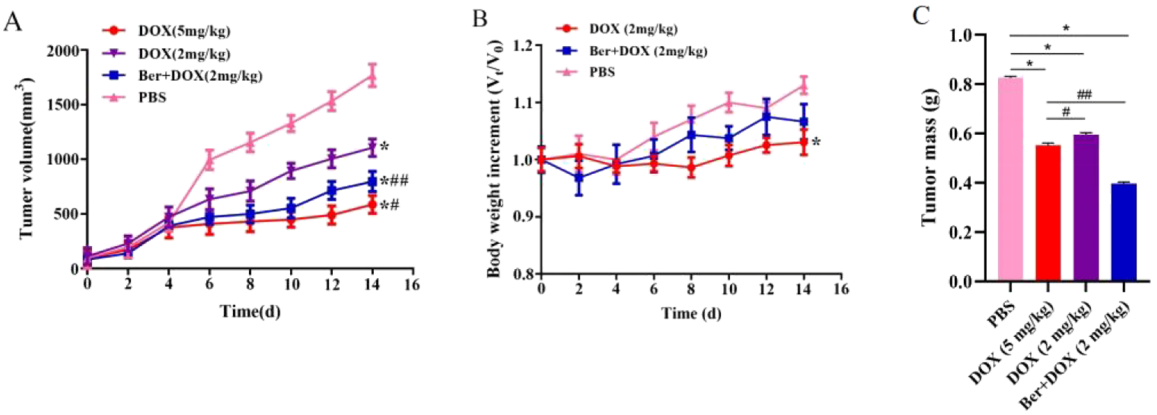

Figure 3. (A) Tumor volumes of MCF-7/DOX^{Fluc} tumor-bearing nude mice treated with DOX (5 or 2 mg/kg, *i.v.*) alone or DOX (2 mg/kg, *i.v.*) combined with Ber (4 mg/kg, *i.p.*). * $P < 0.05$ vs the PBS group; $^{\#}$ $P < 0.05$, $^{\#\#}$ $P < 0.01$ vs the DOX group. (B) Body weight of MCF-7/DOX^{Fluc} tumor-bearing nude mice after being treated with DOX or its combination with Ber. * $P < 0.05$ vs the PBS group. (C) Tumor mass of MCF-7/DOX^{Fluc} tumor-bearing nude mice after being treated with DOX or its combination with Ber. * $P < 0.05$ vs the PBS group; $^{\#}$ $P < 0.05$, $^{\#\#}$ $P < 0.01$ vs the DOX group. Significant differences were assessed using one-way ANOVA. Multiple comparisons between the groups were performed using the Tukey method. Results are presented as means ± SD.

bioluminescence signal of the Ber group was stronger than that of the PBS group (Figure 4B−D). The PK parameters were calculated according to the noncompartmental model. The AUC of the Ber group was higher than that of the PBS group with lower MRT, which meant that Ber can enhance the uptake of D-luciferin potassium salt by tumor cells and reduce the efflux to a certain extent (Table 2).

2.7. Combination of Ber and DOX Had No Obvious Toxicity to Main Organs in Mice. The results of histopathological sections after hematoxylin and eosin (H&E) staining showed that the cells of each organ in the PBS group were closely arranged, the nucleus was complete, the tumor cells were dense, and there was almost no apoptosis or necrosis. Compared with the PBS group, the gap between myocardial cells became larger and the cell morphology changed significantly in the DOX group. The density of nuclei in tumor cells decreased significantly, and some tumor cells died of apoptosis and necrosis. In the Ber + DOX group, the morphology of myocardial cells changed significantly too, which meant that Ber could not reduce the toxic reaction caused by DOX at a high dose. Fortunately, compared with the DOX group, the area of apoptosis and necrosis of tumor cells increased and the nuclei decreased significantly (Figure 5A).

Furthermore, biochemical indexes, such as blood urea nitrogen, creatinine, alanine amino transaminase, and aspartate transaminase were also assessed. There were no significant differences among all groups (Figure 5B).

2.8. Ber Could Increase the Distribution of DOX in Tumor Tissue. After intravenous injection, the distribution of DOX in tumor tissues at 0.5, 2, and 4 h was measured by high-performance liquid chromatography (HPLC). Compared with the DOX group, the Ber + DOX group significantly increased DOX uptake at tumor sites after 0.5, 2, and 4 h (Figure 5C).

2.9. Ber Could Reduce the Expression of P-Gp and MDR Proteins *In Vitro* and *In Vivo*. The results of western blot analysis showed that Ber could downregulate the expression of P-glycoprotein (P-gp) and multidrug resistance protein 1 (MRP1), which indicated that the ability of Ber in reversing drug resistance was partly related to the quantity of key proteins (Figure 6A,B).

The results of IHC experiments showed that the expression of P-gp and MRP1 in the DOX group was significantly upregulated when compared with the PBS group, whereas it was significantly downregulated in the DOX + Ber group (Figure 6C).

The emergence of MDR during chemotherapy is an important reason that restricts clinical treatment and leads to chemotherapy failure. P-gp and MRP1, both of which belong to the ABC transporter family, can combine with chemotherapeutic drugs and pump intracellular drugs to extracellular cells based on the energy released by ATP hydrolysis, thus inducing MDR.[27−30] As an adjuvant drug for chemotherapy, TCM has been proven to be effective in reversing MDR by downregulating the expression of ABC transporters in tumor cells. For example, Yanhusuo can effectively reverse the drug resistance of adriamycin and mitoxantrone by inhibiting P-gp, reducing MRP1-mediated efflux, and activating ATPase activity.[31] Quercetin can significantly improve the chemotherapy effect, and its main mechanism is to downregulate the expression of P-gp and MRP1, increasing the accumulation of DOX in cells and improving the therapeutic effect of DOX.[32] A lot of papers reported the MDR reversal ability by Ber, with an emphasis on its mechanism. For example, Ber could enhance the drug sensitivity and induce apoptosis of breast cancer through different doses of regulation of AMPK signaling pathway. A Low-dose Ber could improve the sensitivity of drug-resistant breast cancer cells to DOX through the AMPK-HIF-1α-P-gp pathway, whereas a high-dose Ber could directly induce apoptosis through the AMPK-p53 pathway.[33] Ber could regulate the expression and function of pgp-170, a gene product of MDR 1, to weaken the response of digestive tract cancer cells to paclitaxel.[34] Ber was also able to slightly upregulate the mRNA levels of MDR1a and MDR1b, thereby affecting the expression and function of MDR proteins.[35] In our research, the MDR reversing mechanism of Ber was studied from both the function and the quantity of the ABC transporter protein. In previous studies related to drug-resistant proteins, people often used flow cytometry and real-time fluorescence quantitative polymerase chain reaction to detect the expression level of drug-resistant proteins.[36,37] The advantage of this method is that it can clearly characterize the cell surface and intracellular protein expression, but it is susceptible to the influence of fluorescence intensity. The relative difference of fluorescence intensity depends on the combination difference of laser and filter on the instrument. Here, with the luciferase reporter gene system combined with

https://doi.org/10.1021/acsomega.0c06288
ACS Omega 2021, 6, 10645−10654

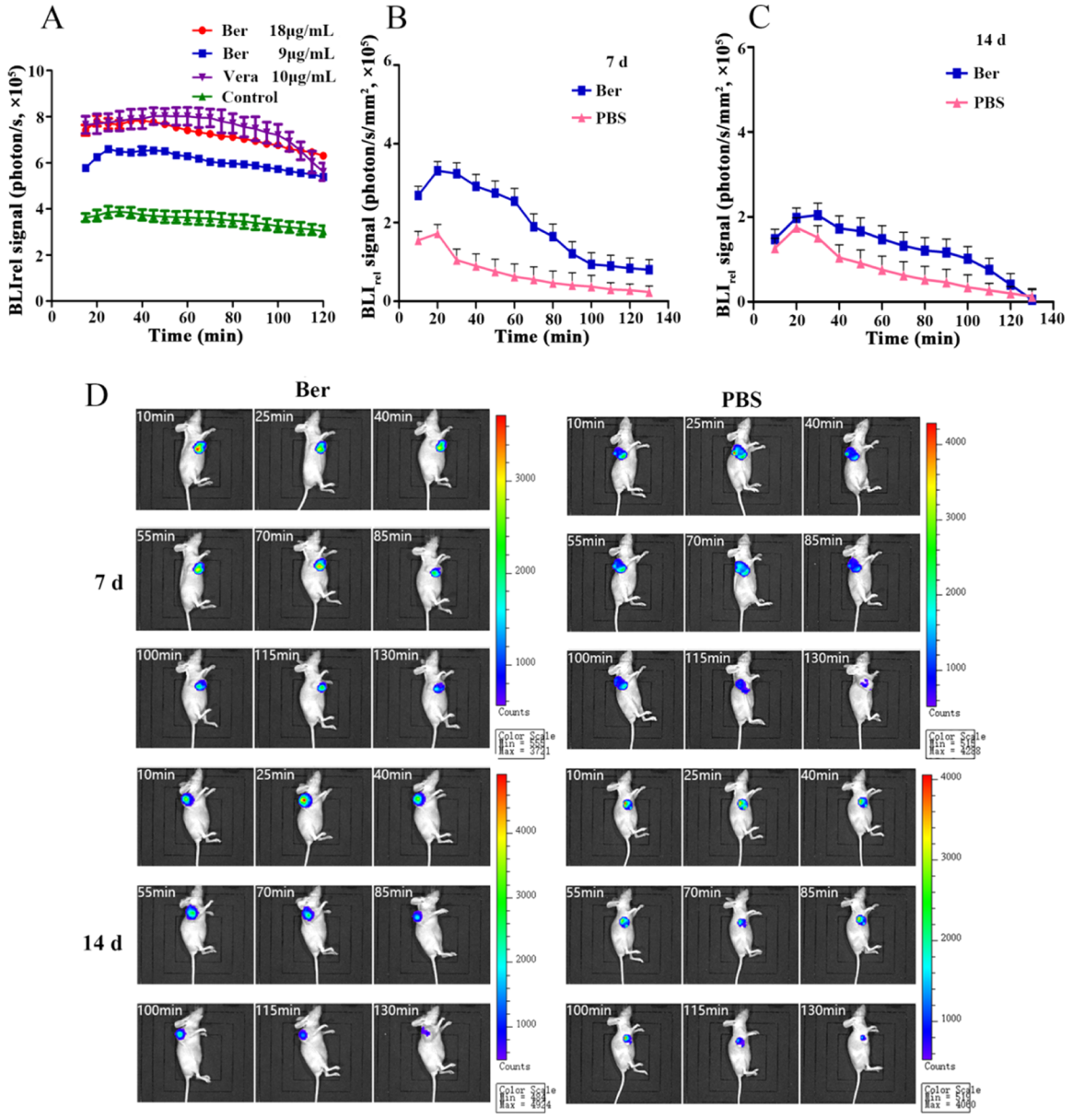

Figure 4. (A) BLI_{rel} signal photon−time curve after being treated with Ber or Vera for 48 h *in vitro*. (B) BLI_{rel} signal photon−time curve of MCF-7/DOX^{Fluc} tumor-bearing nude mice after being treated with Ber for 7 d. (C) BLI_{rel} signal photon−time curve of MCF-7/DOX^{Fluc} tumor-bearing nude mice after being treated with Ber for 14 d. (D) BLI of MCF-7/DOX^{Fluc} tumor-bearing nude mice at different time points within 130 min after being intraperitoneally injected with D-luciferin potassium salt at the dose of 10 mg/kg.

Table 1. Effect of Vera and Ber on the PK Parameters of D-Luciferin Potassium Salt[a]

group	$t_{1/2}$ (min)	MRT (min)	C_{max} (×10^6) (photon/s)	$AUC_{0-120min}$ (×10^8) photon/s*min
Ber (9 μg/mL)	237.03 ± 53.41	254.59 ± 68.54	6.73 ± 0.24***	6.36 ± 0.13***
Ber (18 μg/mL)	264.79 ± 60.78	270.73 ± 71.61	7.82 ± 0.22***	8.16 ± 0.35***
Vera	480.24 ± 81.58	211.43 ± 90.25	8.03 ± 0.29***	8.33 ± 0.37***
PBS	191.94 ± 49.83	289.41 ± 70.53	3.88 ± 0.30	3.97 ± 0.18

[a]Compared with the PBS group, * $P < 0.05$, ** $P < 0.01$, *** $P < 0.001$ ($x \pm s$, $n = 6$).

Table 2. PK Parameters of Treatment with Ber *In Vivo*[a]

	MRT		AUC	
group	7 d	14 d	7 d	14 d
PBS	45.78 ± 0.41	41.32 ± 0.63	84.40 ± 0.78	98.67 ± 0.52
Ber (10 mg/kg)	37.77 ± 0.52	36.59 ± 0.18	196.15 ± 0.83**	142.34 ± 0.47*

[a]Note: Compared with the PBS group, * $P < 0.05$, ** $P < 0.01$.

https://doi.org/10.1021/acsomega.0c06288
ACS Omega 2021, 6, 10645−10654

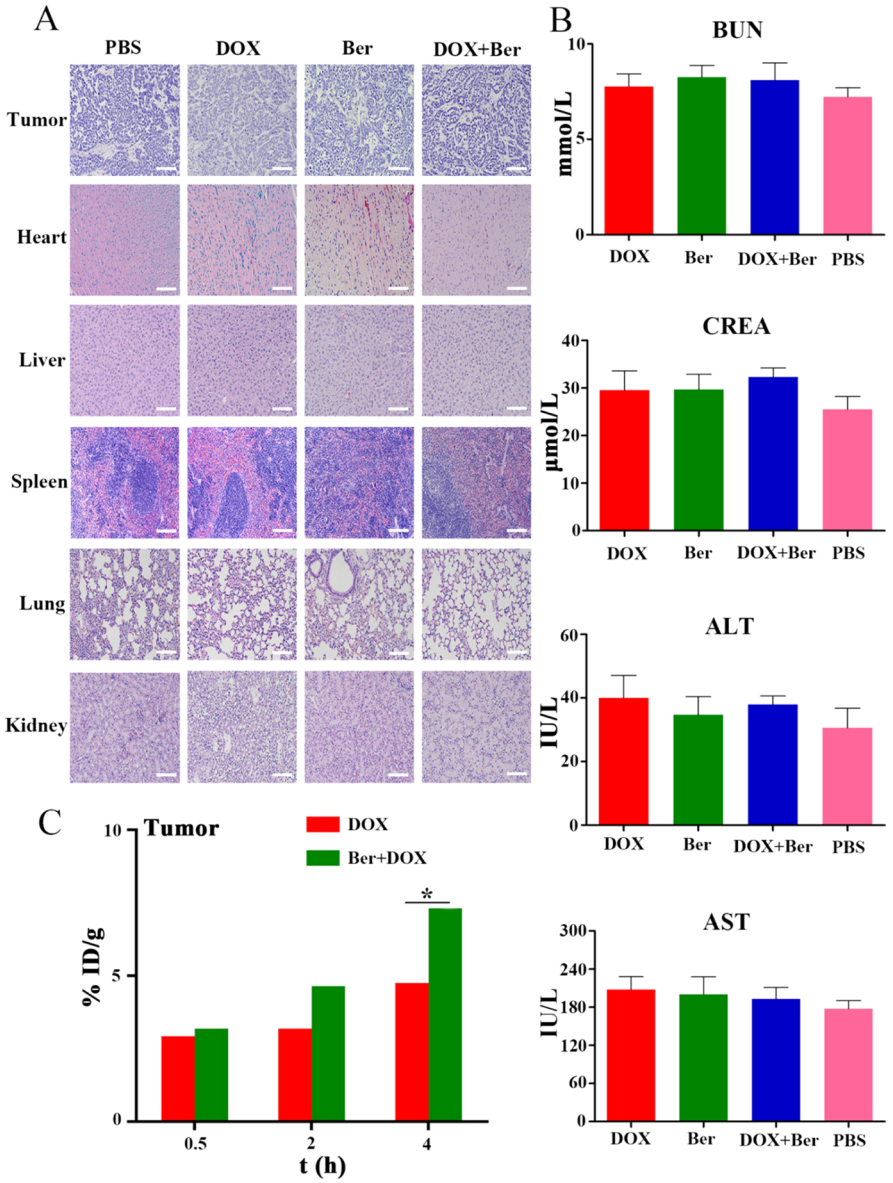

Figure 5. (A) H&E staining of major tissue and tumor taken from MCF-7/DOX^{Fluc} tumor-bearing nude mice after different treatments (200×). Scale bar = 200 μm. (B) Blood biochemical indicators of tumor-bearing nude mice after different treatments. DOX (5 mg/kg, *i.v.*) and Ber (10 mg/kg, *i.p.*). * $P < 0.05$ vs the PBS group. (C) Distribution of DOX in tumor tissue treated by DOX alone or in combination with Ber after 0.5, 2, and 4 h. Significant differences were assessed using the *t* test. Results are presented as means ± SD.

BLI, we established a method for detecting the ABC transporter substrate content in tumor cells by a real-time quantitative and dynamical way *in vivo* and *in vitro*. To study the efflux function caused by the ABC protein, Rhodamine 123 was always used as a marker, which could not be dynamically tracked in real time, especially *in vivo*. D-luciferin potassium is a specific substrate for the ABC transporter. When the intracellular luciferase enzyme is unsaturated, the bioluminescent intensity will follow a linear correlation with the content of D-luciferin potassium salt in cells.[38,39] It provides the possibility to establish a relationship between the pharmacokinetical parameters of fluorescence *in vivo* and *in vitro*. Our results showed that, in the Ber group, there was a positive correlation between the *in vitro* and *in vivo* AUC of the fluorescence in tumor cells, and the Pearson correlation coefficient values were more than 0.7 ($P < 0.05$) (Table 3). This means that the AUC of fluorescence has a strong *in vitro*−*in vivo* correlation. Therefore, it is feasible to screen MDR reversal agents *in vitro* by using the luciferase reporter gene system combined with BLI.

3. CONCLUSIONS

In this work, Ber was demonstrated as an ideal MDR reversing agent. The MDR reversal effect is achieved by inhibiting P-gp and MRP1 functions and their expression in MCF-7/DOX^{Fluc} tumor cells. When combininging Ber with DOX to treat DOX-resistant breast cancer, Ber enhanced the intracellular concentration and retention of DOX in tumor cells, which occurred *via* facilitating the cellular drug uptake and reducing the drug efflux rate in MCF-7/DOX^{Fluc} tumor cells. The DOX−Ber combination significantly enhanced the *in vivo* anticancer efficacy of DOX in a drug-resistant MCF-7/DOX^{Fluc} xenograft model.

https://doi.org/10.1021/acsomega.0c06288
ACS Omega 2021, 6, 10645−10654

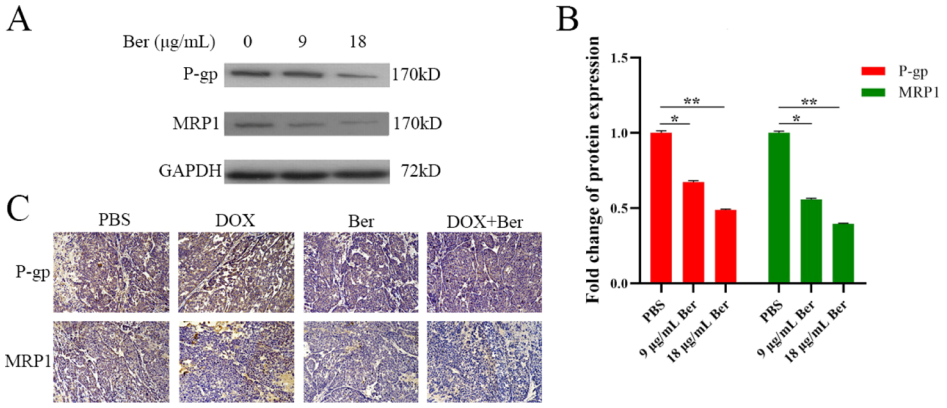

Figure 6. (A) Western blot analysis of P-gp, MRP1 expression. (B) Quantitative analysis of protein expression of western blot. * $P < 0.05$, ** $P < 0.01$ vs the PBS group. (C) IHC staining of tumor taken from MCF-7/DOX^{Fluc} tumor-bearing nude mice after different treatments (200×). Scale bar = 200 μm. P-gp and MRP1 were quantified; a minimum of three randomly selected sample data were quantitatively analyzed using image J software. Significant differences were assessed using the *t* test. Results are presented as means ± SD.

Table 3. Correlation between Tumor Inhibition Rate and AUC after Treatment with Ber *In Vitro* and *In Vivo*

group	Pearson coefficient	*P*
Ber	0.968	0.047

4. EXPERIMENTAL SECTION

4.1. Materials. DOX was purchased from Hisun Pfizer (Hangzhou, China). Ber was obtained from Macklin Biochemical Co., Ltd. (Shanghai, China, purity ≥ 97%). Fetal bovine serum (FBS), penicillin/streptomycin, and trypsin were purchased from Gibco Corporation (USA); D-luciferin potassium salt was provided by Science Light Biology Science & Technology Co., Ltd. (Shanghai, China). Both methyl thiazolyl tetrazolium (MTT) and dimethyl sulfoxide (DMSO) were bought from Sigma-Aldrich (St. Louis, MO, USA). Bicinchoninic acid (BCA) kit and radioimmunoprecipitation assay buffer were purchased from Beyotime Biotechnology (Shanghai, China). Vera was purchased from Apexbio (Houston, USA). Primary antibodies such as P-gp/ABCB1, MRP1/ABCC1, and secondary antibodies were purchased from Abcam Corporation. All chemicals were of analytical reagent grade.

4.2. Cell Lines and Experimental Animals. The MCF-7/DOX human breast cancer cells were kindly provided by West China Pharmacy School of Sichuan University and routinely cultured using RMPI 1640 (from Gibco, USA), supplemented with 10% FBS and 1% penicillin/streptomycin (from Gibco, USA) at 37 °C with 5% CO_2 atmosphere in a humidified incubator. The MCF-7/DOX^{Fluc} cell line, stably expressing the Fluc reporter gene, was constructed by lentivirus infection as in our former studies.[39]

Female BALB/c nude mice (4 weeks old, weighing 18−22 g) were purchased from Slake Laboratory Animal Company (Shanghai, China) and bred by Laboratory Animal Center at Zhejiang Chinese Medical University (Hangzhou, China). To establish the xenograft models, 6×10^7 of MCF-7/DOX^{Fluc} cells and Matrigel (from BD Biosciences, USA) were suspended in PBS at a ratio of 1:1 (v/v) and subcutaneously inoculated on the right side of each mouse. All procedures involving animal experiments were performed in accordance with the protocols approved by the Institutional Animal Care and Use Committee of Zhejiang Chinese Medical University.

4.3. Determination of Multiple Drug Resistance of MCF-7/DOX^{Fluc}. A standard MTT assay was applied to calculate the multiple drug resistance of MCF-7/DOX^{Fluc}. DOX with concentrations of 0.05, 0.10, 0.50, 1.00, and 10.00 μg/mL was applied to MCF-7, and DOX with concentrations of 0.10, 1.00, 10.00, 50.00, and 100.00 μg/mL was applied to MCF-7/DOX^{Fluc}. After incubation at 37 °C for 4 h, the MTT-containing culture medium was discarded, and then 150 μL of DMSO was added. The absorbance of each well was read at 490 nm using a microplate reader (Bio-Tek, USA). Each sample was repeated in triplicate. Cell viability was calculated by the following equation: cell viability (%) = $\{(OD_{sample} - OD_{blank})/(OD_{control} - OD_{blank})\} \times 100\%$. The tumor cell proliferation rate and half-maximal inhibitory concentration (IC_{50}) values were calculated by CompuSyn software. Multiple drug resistance = IC_{50} of MCF-7/DOX^{Fluc}/IC_{50} of MCF-7.

4.4. *In Vitro* Cell Viability Studies. A standard MTT assay was applied to evaluate the MCF-7/DOX^{Fluc} cell cytotoxicity and MDR reversal effect of Ber. MCF-7/DOX^{Fluc} cells were seeded into 96-well plates at a density of 8×10^3 cells per well, 24 h prior to drug treatment. *In vitro* experiments were set up into four groups (PBS group, DOX group, Ber group, and Ber + DOX group), and each group was set up with six wells. The DOX-containing culture medium was added to each well of the DOX group, so that the final concentrations of DOX were 62.50, 31.25, 16.13, 7.813, 3.906, 1.953, 0.9766, 0.4883, and 0.04883 μg/mL. The Ber-containing culture medium was added to each well of the Ber group, so that the final concentrations of Ber were 125.0, 62.50, 31.25, 16.13, 7.813, 3.906, 1.953, 0.9766, and 0.09766 μg/mL. The culture medium containing Ber and DOX was added to each well of the Ber + DOX group, so that the final concentrations of DOX were 62.50, 31.25, 16.13, 7.813, 3.906, 1.953, 0.9766, 0.4883, and 0.04883 μg/mL, and the final concentrations of Ber were adjusted according to the concentrations of DOX, so that the combined ratios of Ber and DOX were 10:1, 5:1, 2:1, and 1:1, respectively. The same volume of culture medium was added to each well in the PBS group. The CI analysis of Ber combined with DOX based on the Chou and Talalay method was conducted using CompuSyn software. For the experimental processing and data analysis, refer to Section 4.3.

4.5. *In Vivo* Antitumor Efficacy and Systemic Toxicity. The xenografts of human breast cancer were used as described in Section 2.2. MCF-7/DOX^{Fluc} tumor-bearing nude mice were

https://doi.org/10.1021/acsomega.0c06288
ACS Omega 2021, 6, 10645−10654

used to evaluate the tumor inhibition efficacy of the different concentrations of Ber in combination with DOX. Ber and DOX were dissolved in PBS. The nude mice were randomized into four groups (n = 6 per group) and treated with PBS, DOX (5 mg/kg, *i.v.*) alone, Ber (10 mg/kg, *i.p.*) alone, and DOX (5 mg/kg, *i.v.*) in combination with Ber (10 mg/kg, *i.p.*). DOX and Ber were administered every other day for 12 days, with a total of six doses. Body weights and tumor volumes were recorded the day after administration. The tumor length (L) and width (W) were used to calculate the volume (V), based on the following equation: $V = (L \times W^2 \times 1/2)$. On every second day post administration, 100 μL of D-luciferin potassium salt (50 mg/kg, dissolved in PBS) was intraperitoneally injected into each group (PBS group, DOX group, Ber group, and Ber + DOX group) and immediately imaged by IVIS (Xenogen, USA) to record the peak value of the fluorescence. The BLI intensity of *in vivo* tumor cells was detected at E_x = 328 nm and E_m = 533 nm. At the end of treatment, the tumors and organs (heart, liver, spleen, lungs, and kidneys) were collected for H&E staining to evaluate specific toxicity.

4.6. *In Vivo* Monitoring of Body Weight and Tumor Volume of MCF-7/DOX^{Fluc} Tumor-Bearing Nude Mice Given Low-Dose DOX. Once the tumors in the tumor-bearing nude mice grew to about 100 mm^3, the mice were randomized into four groups (n = 6 per group) and treated with PBS, DOX (5 mg/kg, *i.v.*) alone, DOX (2 mg/kg, *i.v.*) alone, and DOX (2 mg/kg, *i.v.*) in combination with Ber (4 mg/kg, *i.p.*). The drug was administered six times in succession every other day, during which the body weights and tumor volumes were recorded every other day. The tumor volume was calculated using the calculation formula described in Section 2.4.

4.7. *In Vitro* Fluorescence Kinetics of D-Luciferin Potassium Salt in MCF-7/DOX^{Fluc} Cell Analysis. To investigate the effect on the function of ABC transporter-mediated efflux by Ber *in vitro*, the efflux of D-luciferin potassium salt in MCF-7/DOX^{Fluc} cells was noninvasively monitored by BLI in real time and quantitatively. Our main aim was to use Ber to decrease the MDR on MCF-7/DOX^{Fluc} but not to kill the cells; Ber of 90% IC_{50} and 45% IC_{50} was selected to carry out the *in vitro* experiment. MCF-7/DOX^{Fluc} cells were inoculated into a 96-well plate with a cell density of 8 × 10^3 cells per well. After attachment for 24 h, the cells were treated with Ber at two different concentrations (9 and 18 μg/mL) for another 48 h. Vera (an inhibitor of ABCB1, 10 μg/mL) alone was used as a positive control. Before detection, D-luciferin potassium salt (10 μg/mL) was added to each well and immediately kinetically imaged using IVIS. Excreted extracellular signals were captured every 5 min, and the kinetics of D-luciferin potassium salt was observed within 130 min. The photon signaling intensity of each group was then normalized by the total protein content as relative BLI (BLI_{rel}) in order to eliminate the confounding influence of the increasing cell populations of photon signaling intensity. The BLI_{rel} versus time curves were plotted. According to the noncompartment model method, the dynamic parameters (AUC and MRT) of D-luciferin potassium salt in cells were calculated.

4.8. *In Vivo* Fluorescence Kinetics of D-Luciferin Potassium Salt in MCF-7/DOX^{Fluc} Cell Analysis. The tumor-bearing nude mice were weighed and intraperitoneally injected with D-luciferin potassium salt (10 mg/kg). The BLI signals of each time point were quantitatively recorded within 130 min to obtain the kinetics of D-luciferin potassium salt *in vivo*. The photon signaling intensity of each time point was normalized by the volume of tumors in each treatment group and considered as BLI_{rel}. To obtain the kinetics of D-luciferin potassium salt under the intervention of Ber (10 mg/kg), the BLI signals were taken at every time point for 0−130 min by using the IVIS kinetic imaging system after being treated with Ber at different time points (7 d and 14 d). The BLI signal was also normalized as above. According to the noncompartment model method, the dynamic parameters (AUC and MRT) of D-luciferin potassium salt in cells were calculated.

4.9. Expression of P-Gp and MRP1 Proteins by Western Blot Analysis *In Vitro*. MCF-7/DOX^{Fluc} cells were inoculated into a 10 cm tissue culture dish with a cell density of 4 × 10^6 cells/mL. The culture medium containing Ber with different concentrations (9 and 18 μg/mL) was given. After 48 h, all cells were washed twice with ice-cold PBS, centrifuged at 14,000 rpm for 15 min, and all supernatants were discarded. A volume of 100 μL of cell lysis buffer containing Protease Inhibitor Cocktail was added to the precipitate and incubated on ice for 30 min, then centrifuged at 14,000 rpm for 15 min, and all supernatant was sucked. The protein concentration of cells in the supernatant was determined by BCA assay. A volume of 50 μL of supernatant was taken from each group, added to 5× protein loading buffer, boiled at 100 °C for 5 min, and run on 8% SDS-PAGE gel, and then the protein was transferred from the gel to the PVDF membrane. TBS-T (1×) was used to prepare 5% nonfat milk, and the cell membrane was sealed for 1 h. At 4 °C, it was incubated with primary antibodies (P-gp and MRP1 antibodies) overnight. The membrane was washed three times with 1× TBS-T and then incubated with secondary antibodies (HRP Affini pure goat antirabbit IgG) for 2 h at room temperature. The quantitative analysis of western blot results was conducted using image J software.

4.10. Expression of P-Gp and MRP1 Proteins by IHC *In Vivo*. All tumor tissues were stored with 4% paraformaldehyde and embedded in paraffin. The sections were deparaffinized in xylene and then hydrated with gradient ethanol. The antigen was recovered by microwave heating. The sections were incubated with 3% hydrogen peroxide (H_2O_2) for 30 min at room temperature to eliminate the activity of endogenous peroxidase. The sections were incubated with 10% normal goat serum for 30 min at room temperature. The sections were incubated with primary antibodies (P-gp and MPR1) overnight at 4 °C. After washing with TBS three times, the sections were incubated with labeled polymer-HRP antimouse (DAKO) secondary antibody for 1 h at room temperature. The sections were then exposed to 3, 3′-diaminobenzidine tetrahydrochloride solution and counterstained with hematoxylin.

4.11. *In Vivo* Distribution of DOX. The tumor-bearing nude mice were randomly assigned into two groups (DOX group and Ber + DOX group) (DOX dose of 5 mg/kg, *i.v.*, Ber dose of 10 mg/kg, *i.p.*). Before the experiment, the tumor-bearing nude mice in each group fasted for 12 h and drank water freely. The tumor-bearing nude mice were separately euthanized at 0.5, 2, and 4 h after treatment, and the tumor tissues of each group were excised, rinsed with 0 °C saline, and dried using a filter paper. The tumor weights were measured and recorded. The tissue samples were homogenized in saline (0.25 g/mL) in an ice bath. Then, 0.5 mL of the homogenate was taken from each tumor tissue and placed in a 1.5 mL centrifuge tube. The samples were extracted with 2 mL of methanol−chloroform (1:4, v/v) mixed solution, vortexed for 5 min, centrifuged at 14,000 rpm for 5 min, and the supernatant was harvested and transferred to a clean tube. The supernatant was dried under

https://doi.org/10.1021/acsomega.0c06288
ACS Omega 2021, 6, 10645−10654

nitrogen at room temperature. A volume of 100 μL methanol−chloroform (1:4, v/v) was used to resuspend the sample. The sample was then vortexed for 2 min and centrifuged at 14,000 rpm for 5 min. The supernatant was collected, and the DOX concentration was measured by HPLC (Waters, USA).

4.12. Statistical Analysis. Statistical analysis was performed using SPSS 22.0 software. Data are represented as mean ± SD. The statistical analysis was determined using one-way ANOVA or the *t* test. Multiple comparison between the groups was performed using the Tukey method. * $P < 0.05$, ** $P < 0.01$, # $P < 0.05$, and ## $P < 0.01$ were considered to indicate a statistically significant difference.

AUTHOR INFORMATION

Corresponding Author

Yang Xiong − *Department of Pharmaceutical Sciences, Zhejiang Chinese Medical University, Hangzhou 311402, China; Academy of Chinese Medical Science, Zhejiang Chinese Medical University, Hangzhou 310053, China;* orcid.org/0000-0002-9508-1987; Phone: +86-571-61768158; Email: xyxnb@126.com; Fax: +86-571-61768136

Authors

Ke Qian − *Department of Pharmaceutical Sciences, Zhejiang Chinese Medical University, Hangzhou 311402, China; Academy of Chinese Medical Science, Zhejiang Chinese Medical University, Hangzhou 310053, China*

Chao-yuan Tang − *Department of Pharmaceutical Sciences, Zhejiang Chinese Medical University, Hangzhou 311402, China; Changxing People's Hospital of Zhejiang, Huzhou 313100, China*

Li-ying Chen − *Department of Pharmaceutical Sciences, Zhejiang Chinese Medical University, Hangzhou 311402, China; Academy of Chinese Medical Science, Zhejiang Chinese Medical University, Hangzhou 310053, China*

Shuang Zheng − *Department of Pharmaceutical Sciences, Zhejiang Chinese Medical University, Hangzhou 311402, China*

Yue Zhao − *Department of Pharmaceutical Sciences, Zhejiang Chinese Medical University, Hangzhou 311402, China; Academy of Chinese Medical Science, Zhejiang Chinese Medical University, Hangzhou 310053, China*

Li-sha Ma − *Department of Pharmaceutical Sciences, Zhejiang Chinese Medical University, Hangzhou 311402, China; Academy of Chinese Medical Science, Zhejiang Chinese Medical University, Hangzhou 310053, China*

Li Xu − *The First Affiliated Hospital of Zhejiang Chinese Medical University, Hangzhou 310006, China*

Lu-hui Fan − *Department of Pharmaceutical Sciences, Zhejiang Chinese Medical University, Hangzhou 311402, China*

Jian-dong Yu − *Department of Pharmaceutical Sciences, Zhejiang Chinese Medical University, Hangzhou 311402, China*

Hong-sheng Tan − *Hongqiao International Institute of Medicine, Shanghai Tongren Hospital/Clinical Research Institute, Shanghai Jiao Tong University School of Medicine, Shanghai 200025, China*

Ya-lan Sun − *Department of Pharmaceutical Sciences, Zhejiang Chinese Medical University, Hangzhou 311402, China*

Li-li Shen − *Department of Pharmaceutical Sciences, Zhejiang Chinese Medical University, Hangzhou 311402, China*

Yang Lu − *Department of Pharmaceutical Sciences, Zhejiang Chinese Medical University, Hangzhou 311402, China*

Qi Liu − *Department of Dermatology, Johns Hopkins University School of Medicine, Baltimore, Maryland 21231, United States*

Yun Liu − *Division of Pharmacoengineering and Molecular Pharmaceutics, Eshelman School of Pharmacy, University of North Carolina at Chapel Hill, Chapel Hill 27599, North Carolina, United States*

Complete contact information is available at: https://pubs.acs.org/10.1021/acsomega.0c06288

Author Contributions

[▽]K.Q. and C.-y.T. contributed equally to this work.

Notes

The authors declare no competing financial interest.

ACKNOWLEDGMENTS

This research was financially supported by the project of the National Natural Science Foundation of China (no. 81774011, no. 81473434, and no. 81704082), General research program of Zhejiang Provincial Department of health (no. 2021KY813), Opening Project of Zhejiang Provincial Preponderant and Characteristic Subject of Key University (Traditional Chinese Pharmacology), and Zhejiang Chinese Medical University (no. ZYAOXZD2019003). The authors appreciate the technical support from the Public Platform of Medical Research Center, Academy of Chinese Medical Science, and Zhejiang Chinese Medical University. Thanks to Sara Musetti for polishing the English language of this manuscript.

REFERENCES

(1) Bray, F.; Ferlay, J.; Soerjomataram, I.; Siegel, R. L.; Torre, L. A.; Jemal, A. Global cancer statistics 2018: GLOBOCAN estimates of incidence and mortality worldwide for 36 cancers in 185 countries. *Ca-Cancer J. Clin.* **2018**, *68*, 394−424.

(2) Yang, Y.; Liu, X.; Ma, W.; Xu, Q.; Chen, G.; Wang, Y.; Xiao, H.; Li, N.; Liang, X.-J.; Yu, M.; Yu, Z. Light-activatable liposomes for repetitive on-demand drug release and immunopotentiation in hypoxic tumor therapy. *Biomaterials* **2021**, *265*, 120456.

(3) Yang, Y.; Yu, Y.; Chen, H.; Meng, X.; Ma, W.; Yu, M.; Li, Z.; Li, C.; Liu, H.; Zhang, X.; Xiao, H.; Yu, Z. Illuminating platinum transportation while maximizing therapeutic efficacy by gold nanoclusters via simultaneous near-infrared-I/II imaging and glutathione scavenging. *ACS Nano* **2020**, *14*, 13536−13547.

(4) Yang, C.-X.; Xing, L.; Chang, X.; Zhou, T.-J.; Bi, Y.-Y.; Yu, Z.-Q.; Zhang, Z.-Q.; Jiang, H.-L. Synergistic Platinum(II) Prodrug Nanoparticles for Enhanced Breast Cancer Therapy. *Mol. Pharm.* **2020**, *17*, 1300−1309.

(5) Sun, Y.; Ma, W.; Yang, Y.; He, M.; Li, A.; Bai, L.; Yu, B.; Yu, Z. Cancer nanotechnology: Enhancing tumor cell response to chemotherapy for hepatocellular carcinoma therapy. *Asian J. Pharm. Sci.* **2019**, *14*, 581−594.

(6) Kamaljeet, K.; Goutam, R.; Saket, C.; Ranjit, S.; Amit, K. G. Chemotherapy with si-RNA and anti-Cancer drugs. *Curr. Drug Delivery* **2018**, *15*, 300−311.

(7) Lu, J. F.; Pokharel, D.; Bebawy, M. MRP1 and its role in anticancer drug resistance. *Drug Metab. Rev.* **2015**, *47*, 406−419.

(8) Barbuti, A.; Chen, Z.-S. Paclitaxel Through the ages of anticancer therapy: exploring its role in chemoresistance and radiation therapy. *Cancers* **2015**, *7*, 2360−2371.

(9) Kibria, G.; Hatakeyama, H.; Harashima, H. Cancer multidrug resistance: mechanisms involved and strategies for circumvention using a drug delivery system. *Arch. Pharmacal Res.* **2014**, *37*, 4−15.

(10) Bekele, R. T.; Venkatraman, G.; Liu, R. Z.; Tang, X.; Mi, S.; Benesch, M. G.; Mackey, J. R.; Godbout, R.; Curtis, J. M.; McMullen, T. P.; Brindley, D. N. Oxidative stress contributes to the tamoxifen-

induced killing of breast cancer cells: implications for tamoxifen therapy and resistance. *Sci. Rep.* **2016**, *6*, 21164.
(11) Hermanson, D. L.; Das, S. G.; Li, Y.; Xing, C. Overexpression of Mcl-1 confers multidrug resistance, whereas topoisomeras IIβ down-regulation introduces mitoxantrone-specific drug resistance in acute myeloid leukemia. *Mol. Pharmacol.* **2013**, *84*, 236−243.
(12) Wang, Y.; Wang, X.; Zhao, H.; Liang, B.; Du, Q. Clusterin confers resistance to TNF-alpha-induced apoptosis in breast cancer cells through NF-kappaB activation and Bcl-2 overexpression. *J. Chemother.* **2012**, *24*, 348−357.
(13) Zhou, D.; Liu, W.; Liang, S.; Sun, B.; Liu, A.; Cui, Z.; Han, X.; Yuan, L. Apoptin-derived peptide reverses cisplatin resistance in gastric cancer through the PI3K-AKT signaling pathway. *Cancer Med.* **2018**, *7*, 1369−1383.
(14) He, W.-t.; Zhu, Y.-h.; Zhang, T.; Abulimiti, P.; Zeng, F.-y.; Zhang, L.-p.; Luo, L.-j.; Xie, X.-m.; Zhang, H.-l. Curcumin reverses 5-fluorouracil resistance by promoting human colon cancer HCT-8/5-FU cell apoptosis and down-regulating heat shock protein 27 and p-glycoprotein. *Chin. J. Integr. Med.* **2019**, *25*, 416−424.
(15) Lin, F.-Z.; Wang, S.-C.; Hsi, Y.-T.; Lo, Y.-S.; Lin, C.-C.; Chuang, Y.-C.; Lin, S.-H.; Hsieh, M.-J.; Chen, M.-K. Celastrol induces vincristine multidrug resistance oral cancer cell apoptosis by targeting JNK1/2 signaling pathway. *Phytomedicine* **2019**, *54*, 1−8.
(16) Tian, L.; Zhang, Y.; Wang, Y.; Dang, R.; Fu, Z.; Gu, B.; Wen, N. Triptolide reduces proliferation and enhances apoptosis in drug-resistant human oral cancer cells. *Int. J. Clin. Exp. Pathol.* **2019**, *12*, 1204−1213.
(17) Zhang, W.; Li, M.; Du, W.; Yang, W.; Li, G.; Zhang, C.; Liang, X.; Chen, H. Tissue distribution and anti-lung cancer effect of 10-hydroxycamptothecin combined with platycodonis radix and glycyrrhizae radix ET rhizoma. *Molecules* **2019**, *24*, 2068−2081.
(18) Su, F.; Wang, J. Berberine inhibits the MexXY-OprM efflux pump to reverse imipenem resistance in a clinical carbapenem-resistant pseudomonas aeruginosa isolate in a planktonic state. *Exp. Ther. Med.* **2018**, *15*, 467−472.
(19) Scarfe, L.; Taylor, A.; Sharkey, J.; Harwood, R.; Barrow, M.; Comenge, J.; Beeken, L.; Astley, C.; Santeramo, I.; Hutchinson, C.; Ressel, L.; Smythe, J.; Austin, E.; Levy, R.; Rosseinsky, M. J.; Adams, D. J.; Poptani, H.; Park, B. K.; Murray, P.; Wilm, B. Non-invasive imaging reveals conditions that impact distribution and persistence of cells after in vivo administration. *Stem Cell Res. Ther.* **2018**, *9*, 332.
(20) Thompson, S. M.; Callstrom, M. R.; Knudsen, B. E.; Anderson, J. L.; Sutor, S. L.; Butters, K. A.; Kuo, C.; Grande, J. P.; Roberts, L. R.; Woodrum, D. A. Molecular bioluminescence imaging as a noninvasive tool for monitoring tumor growth and therapeutic response to MRI-guided laser ablation in a rat model of hepatocellular carcinoma. *Invest. Radiol.* **2013**, *48*, 413−421.
(21) Close, D. M.; Xu, T.; Sayler, G. S.; Ripp, S. In vivo bioluminescent imaging (BLI): noninvasive visualization and interrogation of biological processes in living animals. *Sensors* **2011**, *11*, 180−206.
(22) Christoph, S.; Schlegel, J.; Alvarez-Calderon, F.; Kim, Y.-M.; Brandao, L. N.; DeRyckere, D.; Graham, D. K. Bioluminescence imaging of leukemia cell lines in vitro and in mouse xenografts: effects of monoclonal and polyclonal cell populations on intensity and kinetics of photon emission. *J. Hematol. Oncol.* **2013**, *6*, 10−19.
(23) Zhang, Y.; Pullambhatla, M.; Laterra, J.; Pomper, M. G. Influence of bioluminescence imaging dynamics by D-luciferin uptake and efflux mechanisms. *Mol. Imaging* **2012**, *11*, 499−506.
(24) Huang, R.; Vider, J.; Serganova, I.; Blasberg, R. G. ATP-binding cassette transporters modulate both coelenterazine- and D-luciferin-based bioluminescence imaging. *Mol. Imaging* **2011**, *10*, 215−226.
(25) Zhang, Y.; Bressler, J. P.; Neal, J.; Lal, B.; Bhang, H.-E. C.; Laterra, J.; Pomper, M. G. ABCG2/BCRP Expression Modulates d-Luciferin-Based Bioluminescence Imaging. *Cancer Res.* **2007**, *67*, 9389−9397.
(26) Close, D. M.; Hahn, R. E.; Patterson, S. S.; Baek, S. J.; Ripp, S. A.; Sayler, G. S. Comparison of human optimized bacterial luciferase, firefly luciferase, and green fluorescent protein for continuous imaging of cell culture and animal models. *J. Biomed. Opt.* **2011**, *16*, 047003−047014.
(27) Liu, S.; Chen, S.; Yuan, W.; Wang, H.; Chen, K.; Li, D.; Li, D. PD-1/PD-L1 interaction up-regulates MDR1/P-gp expression in breast cancer cells via PI3K/AKT and MAPK/ERK pathways. *Oncotarget* **2017**, *8*, 99901−99912.
(28) Shapira, A.; Livney, Y. D.; Broxterman, H. J.; Assaraf, Y. G. Nanomedicine for targeted cancer therapy: Towards the overcoming of drug resistance. *Drug Resist. Updates* **2011**, *14*, 150−163.
(29) Zhang, H.; Fu, L. W. Multidrug resistance-associated proteins and their roles in multidrug resistance. *Acta Pharmacol. Sin.* **2011**, *46*, 479−486.
(30) Lei, Y.; Tan, J.; Wink, M.; Ma, Y.; Li, N.; Su, G. An isoquinoline alkaloid from the Chinese herbal plant corydalis yanhusuo W.T. Wang inhibits p-glycoprotein and multidrug resistance-associate protein 1. *Food Chem.* **2013**, *136*, 1117−1121.
(31) He, Z.; Xiao, X.; Li, S.; Guo, Y.; Huang, Q.; Shi, X.; Wang, X.; Liu, Y. Oridonin induces apoptosis and reverses drug resistance in cisplatin resistant human gastric cancer cells. *Oncol. Lett.* **2017**, *14*, 2499−2504.
(32) Pan, Y.; Zhang, F.; Zhao, Y.; Shao, D.; Zheng, X.; Chen, Y.; He, K.; Li, J.; Chen, L. Berberine enhances chemosensitivity and induces apoptosis through dose-orchestrated AMPK signaling in breast cancer. *J. Cancer* **2017**, *8*, 1679−1689.
(33) Lin, H.-L.; Liu, T.-Y.; Wu, C.-W.; Chi, C.-W. Berberine modulates expression of mdr1 gene product and the responses of digestive track cancer cells to paclitaxel. *Br. J. Cancer* **1999**, *81*, 416−422.
(34) Hiroka, S.; Hiroki, T.; Hajime, M.; Makoto, I. Selective regulation of multidrug resistance protein in vascular smooth muscle cells by the isoquinoline alkaloid coptisine. *Biol. Pharm. Bull.* **2010**, *33*, 677−682.
(35) Cheng, J.; Dai, J. Y.; Chen, B. A.; Cai, X. H.; Wang, S.; Gao, F. Mechanisms of tetrandrine and 5-bromotetrandrine in reversing multidrug resistance may relate to down-regulation of multidrug resistance associated protein 7 expression. *J. Exp. Hematol.* **2012**, *20*, 558−563.
(36) Xu, W.-l.; Jiang, Y. w.; Wang, F. c. Reversal mechanism of multidrug resistance in leukemia cell line K562/ADM. *Practical J. Cancer.* **2003**, *18*, 347−349.
(37) Sun, Y.; Gu, M.; Zhu, L.; Liu, J.; Xiong, Y.; Wei, Y.; Li, F. Gemcitabine upregulates ABCG2/BCRP and modulates the intracellular pharmacokinetic profiles of bioluminescence in pancreatic cancer cells. *Anticancer Drugs* **2016**, *27*, 183−191.
(38) Rettig, G. R.; Mcanuff, M.; Liu, D.; Kim, J.-S.; Rice, K. G. Quantitative bioluminescence imaging of transgene expression in vivo. *Anal. Biochem.* **2006**, *355*, 90−94.
(39) Tang, C.-y.; Zhu, L.-x.; Yu, J.-d.; Chen, Z.; Gu, M.-c.; Mu, C.-f.; Liu, Q.; Xiong, Y. Effect of β-elemene on the kinetics of intracellular transport of d-luciferin potassium salt (ABC substrate) in doxorubicin-resistant breast cancer cells and the associated molecular mechanism. *Eur. J. Pharm. Sci.* **2018**, *120*, 20−29.

https://doi.org/10.1021/acsomega.0c06288
ACS Omega 2021, 6, 10645−10654